

PHYSICAL REVIEW C **79**, 024311 (2009)

# Half-life of the superallowed positron emitter $^{10}\text{C}$

P. H. Barker and K. K. H. Leung

*Physics Department, University of Auckland, Private Bag 92019, Auckland, New Zealand*

A. P. Byrne

*Department of Nuclear Physics, RSPHYSE and Physics Department, Australian National University, Canberra, Australia*

(Received 18 July 2008; published 17 February 2009)

The half-life of the nucleus  $^{10}\text{C}$  has been determined by detecting its decay positrons in an  $E$ - $\Delta E$  fast scintillator telescope and recording the data in event mode. Care was taken to exclude the effects of possible contaminant activities and of pileup in the linear electronic systems. A value of 19.282(11) s has been obtained, which is in good agreement with two of the three previous measurements, but not with the most recent.

DOI: [10.1103/PhysRevC.79.024311](https://doi.org/10.1103/PhysRevC.79.024311)

PACS number(s): 21.10.Tg, 23.40.-s, 27.20.+n

## I. INTRODUCTION

The importance of determining the  $\mathcal{F}t$  values of superallowed  $0^+ \rightarrow 0^+$ ,  $T = 1$  positron decays with high precision has been emphasized in a recent compilation of the experimental results which form the database from which the values are calculated [1]. As discussed there, conclusions pertaining to the conserved vector current theory and the unitarity of the Cabibbo-Kobayashi-Maskawa (CKM) weak interaction matrix may be drawn from such a study.

Of the positron decays discussed in Ref. [1], nine  $\mathcal{F}t$  values, ranging from that of  $^{10}\text{C}$  to that of  $^{54}\text{Co}$ , are quoted to a precision of 0.2% or better, and the constancy of these values as the charge of the final nucleus,  $Z$ , varies from 5 to 26 is a powerful support of the underlying theory and a means of setting limits on the occurrence of as yet undetected phenomena, as discussed in detail in Ref. [1]. Since many of the theoretical steps that lead to the calculation of a final  $\mathcal{F}t$  from the raw experimental results depend on  $Z$ , their validity is particularly tested for the extreme case of  $^{10}\text{C}$  decaying to  $^{10}\text{B}$ , with  $Z = 5$ , which is the lightest of the nine decaying nuclei.

Three experimental quantities are needed to calculate an  $\mathcal{F}t$  value: the positron maximum energy, the branching ratio of the superallowed component of the decay, and the half-life. For  $^{10}\text{C}$ , the defining measurements of each of these, as summarized in Ref. [1], are perhaps not as satisfactory as could be wished. The energy has been measured twice [2,3], and the values are in good agreement, but they do come from the same laboratory, using essentially the same technique, albeit considerably improved for the later result.

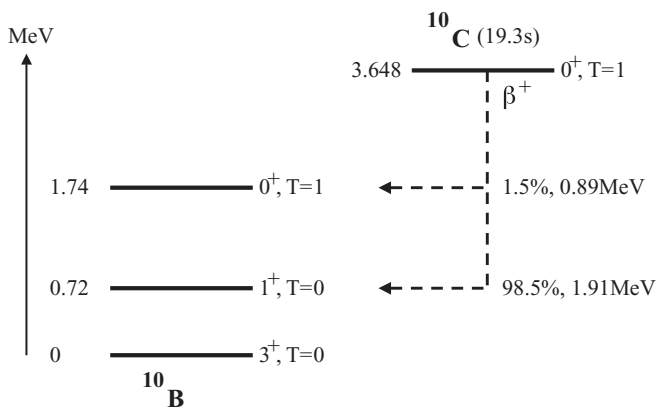
The branching ratio is a very small percentage, which is difficult to determine with the desired accuracy. In addition, it comes from two experiments employing the same basic idea, Refs. [4,5], although they were performed in different laboratories. In such a measurement, where the two  $\gamma$  rays that follow the  $^{10}\text{C}$   $\beta$  decays are detected using germanium detectors and their relative intensity must be determined, a critical aspect is establishing the relative detection efficiency of the system. Whereas in a recent superallowed  $\beta$ -decay half-life measurement, that of  $^{22}\text{Mg}$  [6], this was accomplished by constructing a curve representing the general dependency of detector

efficiency on  $\gamma$  energy, in Refs. [4,5] an ingenious method was employed in which the two  $\gamma$  rays of interest were produced in equal numbers in a separate experiment, and their detected numbers gave the desired relative efficiency directly. While this latter method is simpler and more powerful, the overall situation would be improved if the branching ratio could be measured again, preferably using a different calibration method.

For the half-life, both results cited in Ref. [1], i.e., 19.280(20) and 19.295(15) s, were obtained in experiments (Refs. [7] and [8], respectively) in which the 717 keV  $\gamma$  ray, which follows each  $^{10}\text{C}$  decay (see Fig. 1), was taken as a unique decay signature to avoid the interference of contaminants, and detected using a high-resolution germanium detector.

In a recent paper [9], we have shown that the use of a germanium detector in experiments in which precise knowledge of the intensity variation over time of a particular  $\gamma$  ray is critical are subject to uncertainties because of possible pileup effects in the analog electronics. In fact, we came to the conclusion that half-life determinations using this technique, which did not specifically discuss the measures used to combat and overcome pileup problems, should be accorded some doubt. We feel that the results cited in Ref. [8], in which one of us is a co-author, perhaps fall into this category, although there is no evidence to indicate the presence of such a problem. For the other, these authors measured five half-lives, Refs. [7,10], but only one other, that of  $^{14}\text{O}$ , involved the use of a germanium detector, and the quoted uncertainty on that result, 0.26%, Ref. [10], is much larger than that on the presently accepted value for  $^{14}\text{O}$ , 0.02%, or for their  $^{10}\text{C}$  result, 0.1%, so it is hard to draw any relevant conclusions. But again, there is no actual evidence of a problem.

The overall effect of pileup on a half-life determination using a  $\gamma$ -ray counting system is hard to predict. Normally by far the strongest source of radiation is from the decay of interest itself. If all the detected radiation is being time-binned and then used to give a half-life value, the most likely random pileup is of a pulse from a decay of half-life say  $T$ , with another, independent but also from such a decay. This effect has been shown to generate pileup that exhibits a half-life of  $T/2$  [11,12]. The case of a narrow region of interest (ROI)

FIG. 1. Positron decay of  $^{10}\text{C}$ .

used as an energy cut in a germanium detector spectrum adds additional complications. If the pileup is of two smaller pulses that add together to finish within the ROI, that pileup will add a component to the ROI decay of half-life  $T/2$ . If the pileup is of a pulse, which would otherwise have been in the ROI, with any other pulse, it will remove a component of half-life  $T/2$  from the ROI contents. It seems therefore that the most reliable way to detect and deal with pileup is to incorporate appropriate tests in the data analysis.

In a recent work [13], an attempt has been made to circumvent these problems by using a combination of a mass separator, to give an unadulterated source of  $^{10}\text{C}$  nuclei, and a fast gas counter to detect the decay positrons. For such a system, pileup problems are straightforward to avoid, but an unexpected small, but not insignificant, source of contaminant activity was identified and had to be taken into account in producing a final half-life value of  $19.310(4)$  s. Unfortunately, this value, while showing a smaller uncertainty than the values of Refs. [7,8], does not sit particularly easily with them, having a normalized chi square of 1.5 for the set. According to the relevant criterion of the Particle Data Group [14], which is also adopted by the authors of Ref. [1], this value gives grounds for concern.

Accordingly, we have sought to measure the half-life of  $^{10}\text{C}$  using different methods of production and detection, in the hope of finally determining whether there is an overall problem.

## II. EXPERIMENTAL METHOD

The  $^{10}\text{C}$  nuclei were produced using the  $^{10}\text{B}(p, n)^{10}\text{C}$  reaction, with protons coming from the 14UD electrostatic accelerator at the ANU Department of Nuclear Physics. The target was  $13\text{ mg/cm}^2$  of boron, specified as 99.95%  $^{10}\text{B}$  and 0.05%  $^{11}\text{B}$  by the manufacturer, on 0.02 mm 99.999% gold backing, with the beam passing through the target and backing to hit a 99.995% gold stopper. After bombarding the target for 60 s (approximately three half-lives of  $^{10}\text{C}$ ), the beam was chopped at the exit of the accelerator ion source, and the target was moved on a magnetically operated arm away from the stopper to in front of a positron telescope; the resulting activity was counted for 400 s.

The telescope consisted of two St Gobain BC400 scintillator discs, 50 mm diameter, the first ( $\Delta E$ ) 1 mm thick and the second ( $E$ ) 15 mm, coupled to Perspex light guides and Hamamatsu R329-02 photomultiplier tubes (PMTs). The telescope looked at the struck side of the target, and a positron leaving the target typically lost 200 keV in reaching the  $E$  detector. The scintillators were shielded from the beam path by 25 mm of lead, although, of course, there was no beam during the actual counting periods.

Output pulses from the PMTs were less than 15 ns long and produced logic pulses from constant fraction discriminators (CFDs) which were 12 ns long, with a time jitter of less than 2 ns. The overlap coincidences from these gave gate pulses 25 ns long, which safely covered the associated  $E$  analog pulses, and gated them. With this analog system and maximum count rates of less than  $1000 \text{ s}^{-1}$ , pileup rates are expected to be completely negligible. Following passage through the gate, the analog pulses were shaped by a slow integrating amplifier with  $0.25 \mu\text{s}$  shaping time, whose unipolar output was completely finished in  $2.1 \mu\text{s}$ , and then passed to a Lecroy 3514 Camac ADC.

In the Camac system, a precision 1-s pulser provided a time standard, and this was zeroed at the start of each count period. Each valid  $E$  output from the telescope was recorded in event mode, along with the elapsed time after the start of the count period. In this mode, the Camac system took  $5.2\ \mu\text{s}$  to process an event. To be able to impose a fixed dead time on the system externally, a system inhibit was generated 17 ns after the start of the fast gate. Its length was measured to be  $6.02(5)\ \mu\text{s}$  using a digital oscilloscope and determined in practice to be  $6.05(1)\ \mu\text{s}$  using a double pulse technique.

The  $\Delta E$ - $E$  fast coincidence requirement did not completely prevent the telescope's registering individual  $\gamma$  rays, as Compton scattering in either detector with the scattered electron being then detected by the other gave a true coincidence. But in a test using a  $^{137}\text{Cs}$  source, the exclusion of  $\gamma$  rays of 662 keV, emanating from the target counting position and registered by the  $E$  scintillator, was 99.7%.

In a half-life determination such as this, an important element, as alluded to earlier, is the avoidance, or eventual detection, of contaminant positron activity from the target. Accordingly, at each stage of the target fabrication, a parallel process produced a sample which was tested in realistic conditions with the beam in the target chamber. Initially, with a proton beam energy of 6.0 MeV, a short-lived activity of half-life 7(3) s was seen by the telescope, which was not unexpected, as the sole quoted light element in the gold backing was 1 ppm of magnesium. Since both  $^{25}\text{Mg}$  [with  $^{25}\text{Mg}(p, n)^{25}\text{Al}(\beta^+)^{25}\text{Mg}$ , maximum positron energy 4.3 MeV, half-life 7.2 s, and proton energy threshold 5.28 MeV] and  $^{26}\text{Mg}$  [with  $^{26}\text{Mg}(p, n)^{26}\text{Al}^m(\beta^+)^{26}\text{Al}$ , maximum positron energy 3.2 MeV, half-life 6.4 s, and proton energy threshold 5.21 MeV] produce such activity, this was avoided by reducing the proton energy to 5.20 MeV. No other positron activity was seen at any stage other than the long-lived  $^{11}\text{C}$  from the 0.05%  $^{11}\text{C}$  via  $^{11}\text{B}(p, n)^{11}\text{C}(\beta^+)^{11}\text{B}$ , maximum positron energy 0.96 MeV, half-life 1223 s, and proton energy threshold 3.0 MeV.

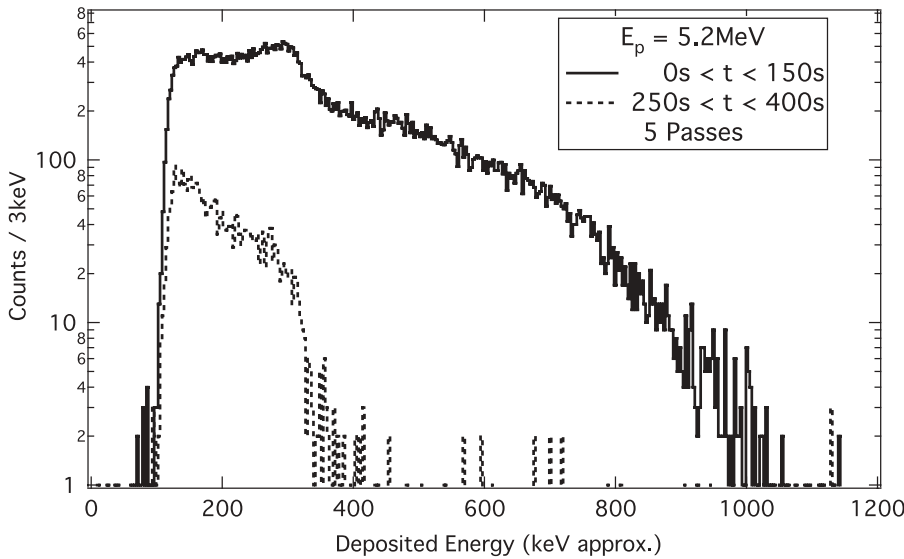


FIG. 2. Energy spectra accumulated during the five passes of a typical run for the first 150 s and the last 150 s of the beam-off periods.

To prevent the positrons from  $^{11}\text{B}$  from reaching the detector telescope, 2.8 mm of Perspex was interposed between it and the target count position. But, as discussed above, the system is not completely inert to  $\gamma$  rays, particularly because for each positron there are two 511 keV annihilation quanta produced, and so there was a small energy component of 1223 s half-life in the data, which was incorporated in the subsequent analysis, as discussed in a later section.

A standard run consisted of five passes, each of which comprised a 60 s beam-on followed by a 400 s beam-off period. Typical beam current intensities of 5.2 MeV protons were 150–300 nA, and initial count rates in the beam-off period ranged up to  $600\text{ s}^{-1}$ . The gated energy spectrum from the  $E$  detector for such a run is shown in Fig. 2, where the energy designation in keV is approximate, but is the same for all energy spectra shown, and was derived from comparing the endpoints of the  $^{10}\text{C}$   $\beta$  spectra with various thicknesses of Perspex interposed between the telescope and the target. In Fig. 2, two spectra are contrasted: that from the first 150 s of the counting periods, which is almost totally from  $^{10}\text{C}$ , and that from the last 150 s, when the  $^{10}\text{C}$  activity, after 13 half-lives, has decayed away. What is apparent is that the expected nonzero contribution from  $^{11}\text{C}$  activity is present in the latter as a low-energy continuum from the Compton interaction of a 511 keV photon in the  $E$  detector, with the scattered photon giving the  $\Delta E$  coincidence.

To search for disturbing contaminants that may be present, the proton beam energy was reduced below the  $^{10}\text{C}$  threshold energy of 4.88 MeV, to 4.80 MeV. The normalized energy spectrum for this case was identical within statistics with the later one of Fig. 2, and so, there being no positron-producing, proton-induced reactions with thresholds between 4.8 and 5.2 MeV, other than the one of interest, we conclude that the only activity whose influence must be included in subsequent analysis is that of  $^{11}\text{C}$ , that its intensity will be very small, and

that its energy spectrum does not extend beyond a nominal 400 keV.

### III. ANALYSIS AND RESULTS

In all, a total of 81 runs were taken, each with five passes, as described above. The runs were in six separate sessions, and so the results are presented as from the six groups, with each individual pass being treated separately. Following the discussion above, as there was no  $^{11}\text{C}$  activity above a nominal 400 keV, the data were analyzed in two statistically independent modes: energy pulses from 401–1200 keV were projected onto the time axis and analyzed in terms of a single exponential and a (very small) constant background; those from 0–400 keV were projected onto the time axis and analyzed in terms of an exponential of unknown half-life, one of half-life 1223 s, and a constant background. The parameters were extracted using the maximum likelihood technique. Each data ordinate was corrected linearly for the  $6.05(1)\text{ }\mu\text{s}$  dead time per pulse of total count rate. To illustrate the process, the analysis of group 6 will be discussed.

Despite our confidence that neither analog pileup nor undetected contaminant activity was influencing our results, we searched for these features by analyzing each pass three times, starting the analysis time at 0, 20, and 40 s, respectively, and plotting the results as a function of the total system count rate at the start of those times. In Fig. 3, this is shown for the 75 passes of group 6,  $E = 401\text{--}1200\text{ keV}$ . A dependency of the extracted half-life on the initial count rate or, alternatively viewed, on the starting time for the analysis would indicate the presence of one of the problems alluded to, but the slope of a straight line fit to the results,  $-0.3(21) \times 10^{-3}\text{ s}^2$ , is statistically zero.

The results of a similar analysis, this time of group 6,  $E = 0\text{--}400\text{ keV}$  time projections, are shown in Fig. 4. Again, there is no dependency of half-life on count rate. Overall,

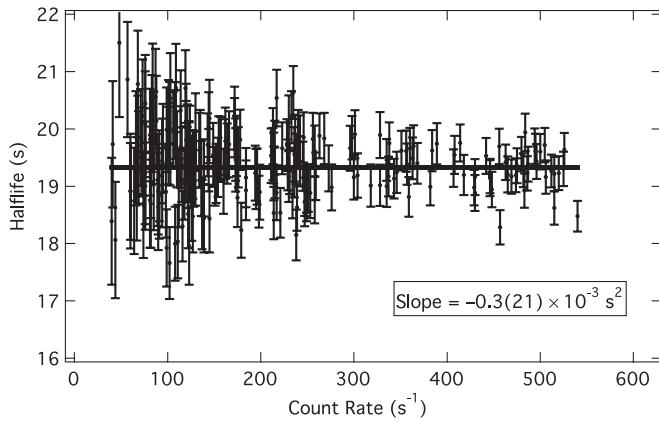


FIG. 3. Time-chopped half-life results for the higher energy projection of the 75 passes of group 6, shown as a function of the total count rate at the start of the analysis periods.

such an analysis applied to the two energy cuts from all six groups combined gave a slope of  $4(4) \times 10^{-5} \text{ s}^2$ , with a chi square per degree of freedom of 1.081, identical to within 0.1% to that from an analysis in terms of merely a constant half-life. This equality means that the assumption that there are no unaccounted-for contaminant or counting rate problems seems warranted.

Of course, the results of an analysis of the type shown in Figs. 3 or 4 may not be used to provide a value for the half-life, as the data of successive time chops are not statistically independent. Figure 5 shows the decay curves for a typical single pass from group 6 for each of the two energy projections. One evident feature is that the proportion of  $^{11}\text{C}$  to  $^{10}\text{C}$  in the lower energy projection is around 0.5%. That ratio varied between 0.3% and 2% for the whole data set, depending on whether a sufficient number of runs had been performed continuously to render the amount of  $^{11}\text{C}$  to be in equilibrium.

The extracted half-lives for the 75 passes of group 6, for both energy projections, are shown in Figs. 6 and 7, again plotted as a function of the initial count rate. The weighted

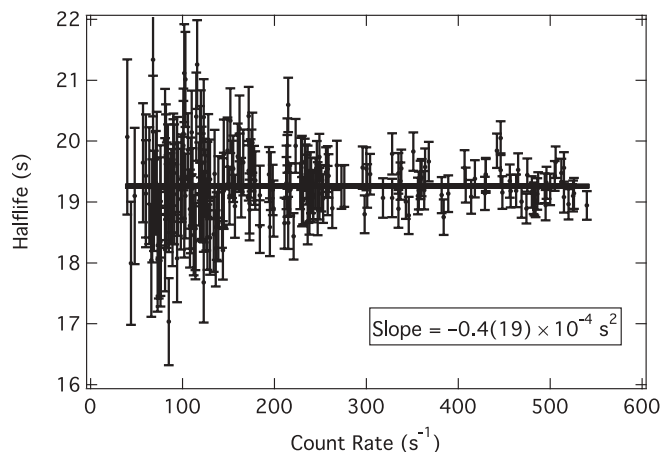


FIG. 4. Same as Fig. 3, but for the lower energy projection.

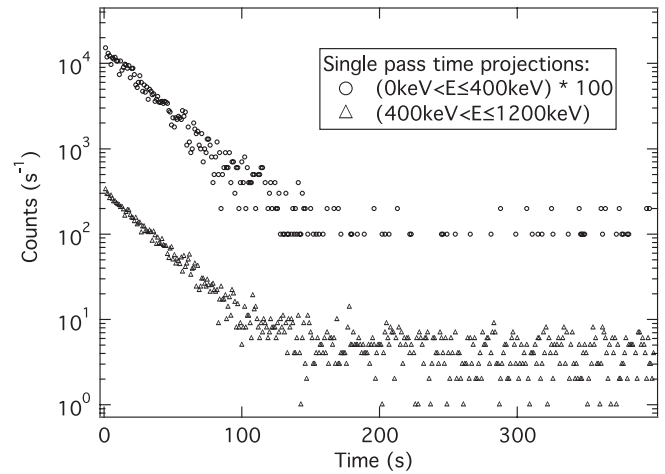


FIG. 5. Typical time projections of a single pass for the low- and high-energy cuts. The former has been increased by a factor of 100 to make it easily distinguishable.

means for the  $^{10}\text{C}$  half-life have acceptable reduced chi-square statistics.

A further test may be applied, in that, if the passes had been performed under identical conditions, the extracted half-life results would have been expected to follow a normal distribution. This is a valuable check that sheds extra light on the results; if the distribution were recognizably not a normal one, that would be a sign that something was amiss, and this would have to be followed up. Figure 8 shows the distribution for the extracted half-lives for both energy cuts of all passes. Although the relative uncertainties on the 810 values range over a factor of 2, so, as stated above, the procedure is formally invalid, the fit to a normal distribution is quite acceptable, and the central half-life is in good agreement with, but does not of course replace, the weighted mean.

The extracted half-lives for all six groups, from both energy projections, are shown in Fig. 9. The results for the two sets are in good accord, both internally and with each other, and lead to an overall value of 19.283 (11) s.

The effect on the  $^{10}\text{C}$  lifetime of the uncertainty in the imposed dead time per pulse cited above is completely

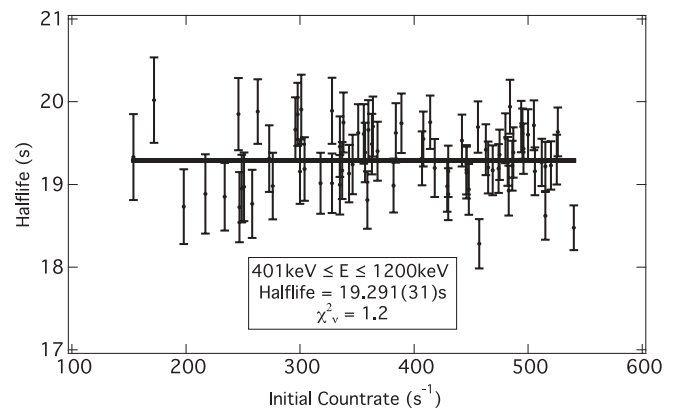


FIG. 6. Extracted half-life values from the higher energy projections of group 6, shown as a function of initial count rate. Also shown is the weighted mean and the reduced chi-square statistic.



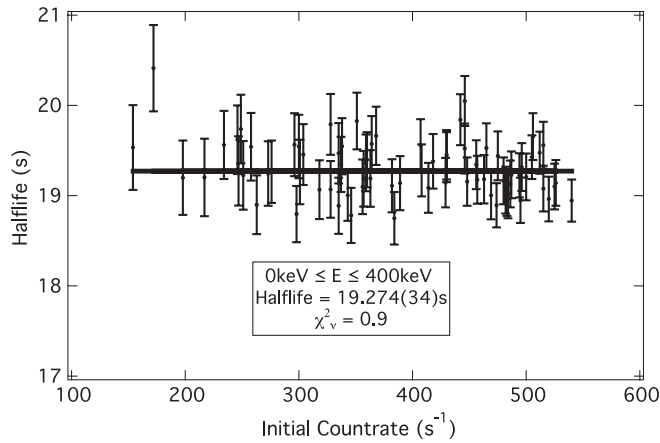


FIG. 7. Same as Fig. 6, but for lower energy projections of group 6.

negligible. Indeed, the count rates encountered, always less than  $600 \text{ s}^{-1}$ , were small enough that the correction for the  $6.05 \mu\text{s}$  dead time itself brought about a change in the half-life of only 18 ms or less. Also completely negligible is the influence of the uncertainty in the  $^{11}\text{C}$  half-life  $1223.1(1.2) \text{ s}$ . In addition, the period of our nominal 1-s clock was measured to be actually  $0.999948 \text{ s}$ , which means the final quoted half-life becomes  $19.282(11) \text{ s}$ , with the ascribed uncertainty coming entirely from the statistical scatter of the individual values.

In a measurement such as this, it is instructive to pose the question, “If the statistical accuracy of the raw data were not the limiting factor, what feature of the experiment would limit the quoted accuracy of the final result?” In the present case, with low count rates and therefore no problems with pileup in the analog systems, the probable answer must lie in the possible presence of a contaminant positron activity, at an intensity level too small to have been detected by the methods discussed above. An activity of half-life comparable with that of  $^{10}\text{C}$ , such as that of  $^{19}\text{Ne}$  from  $^{19}\text{F}(p,n)^{19}\text{Ne}$ , with threshold energy 4.2 MeV, maximum positron energy

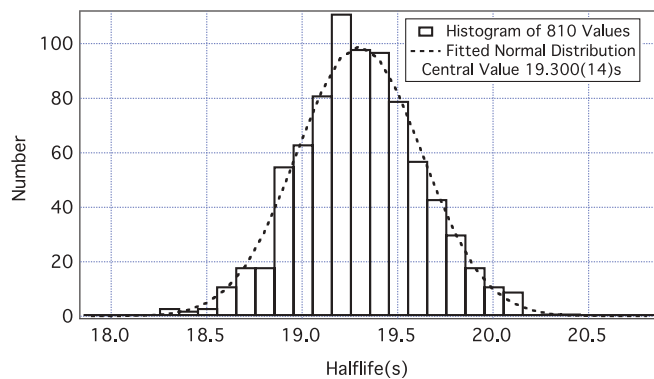


FIG. 8. Histogram of the half-life values extracted from both energy projections of all the passes from all the six groups. Also shown is a fit to a normal distribution.

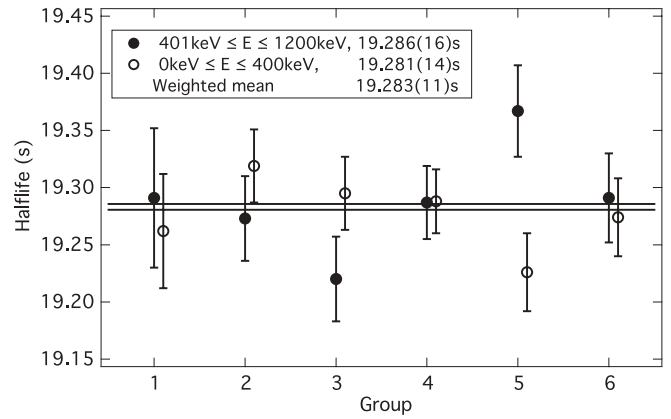
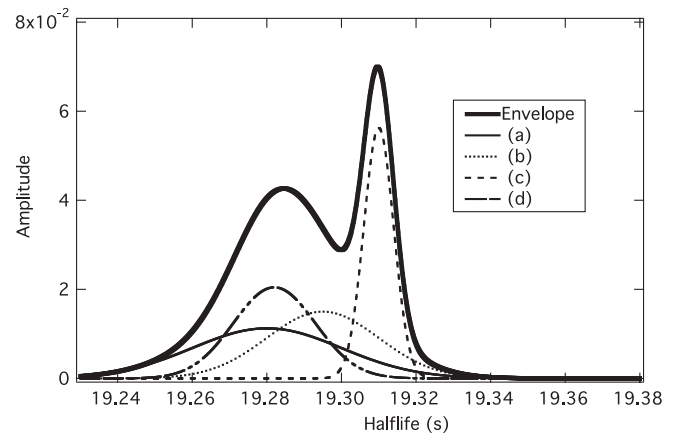


FIG. 9. Results from both energy projections for all six groups, with the weighted means and the overall weighted mean.

2.2 MeV, and half-life 17.5 s, would be hardest to discover. Accordingly, we have taken the largest undetectable intensity of  $^{19}\text{Ne}$  and simulated its effect on the analysis of our data. The result would be to reduce the  $^{10}\text{C}$  half-life by approximately 0.4 ms, which is negligible on the scale of our quoted uncertainty.

#### IV. DISCUSSION

Combining the present half-life result with those from Ref. [1] gives a weighted mean of  $19.285(8) \text{ s}$ , with a chi-square statistic of 0.6, but when the recent result of Ref. [13] is included, the mean becomes  $19.305(4) \text{ s}$ , with a chi-square statistic of 7.8 for three degrees of freedom. Standard statistical analysis indicates that there is only a 5% probability that a consistent set would have a chi square as large as or larger than this, and this is obviously an unsatisfactory position to have arrived at. An attempt to visualize the situation and one which is often used by the authors of Ref. [1], is given in Fig. 10. This is an ideograph, in which each of the four results is

FIG. 10. An ideograph (see text) representing the four results for the half-life of  $^{10}\text{C}$ . (a) Ref. [7], (b) Ref. [8], (c) Ref. [13], and (d) present study.

represented by a normal curve of unit area, with mean equal to the value and width equal to the standard deviation. The shape of the envelope reflects the presence of possible underlying problems.

In Ref. [13], a recommended half-life of 19.308(4) s is used to explore the consequences of the corresponding raising of the  $^{10}\text{C}$   $\mathcal{F}t$  value to 3077.4(46) s, which makes it somewhat higher than the average for the well-known superallowed transitions [1]. In light of our present result, this direction

seems premature and should perhaps await further progress in measurement of the  $^{10}\text{C}$  half-life.

#### ACKNOWLEDGMENTS

The authors thank the staff of the Department of Nuclear Physics at the ANU, Canberra, for their ongoing warm hospitality and assistance.

- 
- [1] J. C. Hardy and I. S. Towner, Phys. Rev. C **71**, 055501 (2005).
  - [2] P. H. Barker and R. E. White, Phys. Rev. C **29**, 1530 (1984).
  - [3] P. H. Barker and P. A. A. Amundsen, Phys. Rev. C **58**, 2571 (1998).
  - [4] B. K. Fujikawa *et al.*, Phys. Lett. **B449**, 6 (1999).
  - [5] G. Savard, A. Galindo-Uribarri, E. Hagberg, J. C. Hardy, V. T. Koslowsky, D. C. Radford, and I. S. Towner, Phys. Rev. Lett. **74**, 1521 (1995).
  - [6] J. C. Hardy, V. E. Iacob, M. S. Sanchez-Vega, R. G. Neilson, A. Azhari, C. A. Gagliardi, V. E. Mayes, X. Tang, L. Trache, and R. E. Tribble, Phys. Rev. Lett. **91**, 082501 (2003).
  - [7] G. Azuelos, J. E. Crawford, and J. E. Kitching, Phys. Rev. C **9**, 1213 (1974).
  - [8] P. H. Barker and G. D. Leonard, Phys. Rev. C **41**, 246 (1990).
  - [9] P. H. Barker, I. C. Barnett, G. J. Baxter, and A. P. Byrne, Phys. Rev. C **70**, 024302 (2004).
  - [10] G. Azuelos and J. E. Kitching, Phys. Rev. C **12**, 563 (1975).
  - [11] D. H. Wilkinson, Nucl. Instrum. **134**, 149 (1976).
  - [12] P. H. Barker, C. J. Scofield, R. J. Petty, J. M. Freeman, S. D. Hoath, W. E. Burcham, and G. T. A. Squier, Nucl. Phys. **A275**, 37 (1977).
  - [13] V. E. Iacob, J. C. Hardy, V. Golovko, J. Goodwin, N. Nica, H. I. Park, L. Trache, and R. E. Tribble, Phys. Rev. C **77**, 045501 (2008).
  - [14] W.-M. Yao *et al.*, J. Phys. G **33**, 1 (2006).